Journal of Solid State Chemistry **158,** 139–147 (2001)
doi:10.1006/jssc.2001.9084, available online at http://www.idealibrary.com on IDEAL®

Unifying Chemical and Physical Principles for Oxide Superconductivity Based on an Anionic Charge Order Model

H. Oesterreicher

Department of Chemistry and Biochemistry, University of California at San Diego, La Jolla, California 92093-0506

Received June 24, 2000; in revised form December 19, 2000; accepted January 19, 2001; published online April 5, 2001

Subperoxidic O_2^{3-} charge ordering presents a satisfying basis for a quantitative, conceptually realistic, and unifying understanding of cuprate superconductors. The activity of O^- manifests itself in a variety of ways including a universal T_c scaling with O^- per total O, or more generally, in the subperoxide radical concentration. Also, a characteristic crystal chemistry of O^- placement is indicated. As an example, trends to preferential O^- occupation of the apical sites are correlated with *c* axis and T_c decreases providing a new crystallographic interpretation of the overdoping question. Generally, subperoxides can be created on overoxidation or through various modes of self doping through lattice pressure-related factors. Accordingly, the role of peranion formation is seen as a most general chemical principle for ameliorating stacking mismatch through electronic liquefaction under internal stress. Cases are discussed (e.g., $YBa_2Cu_3O_{6.5}$) where the tension on cooling can result in stratified self-doping steps. A variety of experiments indicating charge order properties, such as stripes and slow charge propagation, are interpreted on the anionic model. Subperoxidic pair formation and charge ordering energetics are discussed. Concepts are further generalized for other cases (e.g., carbides or nitrides) of anionic metallicity and superconductivity. Common aspects are mobile, paired charge orders of radicals coupled through bond polarizations. © 2001 Academic Press

INTRODUCTION

General Aspects of the Anionic Model

The nearly 100-year-old quest for a predictive formalism for superconductivity has recently received surprisingly straightforward answers in terms of chemical concepts (1–5). Within the simple overoxidized superconducting cuprates it is found that T_c scales universally with stoichiometric holes (*h* or O^-) distributed per total O. More generally, this corresponds to a radical concentration (*r*) of *p* electrons. The levels and limits (e.g., T_c plateaus) of overoxidation follow straightforward charge order rules. The algorithm also works similarly for complex (e.g., with M = Bi, Hg, Tl) cuprates under the concept of "quantized" self-doping levels. These levels reflect the magnitude of lattice pressure and provide the first quantitative basis for the self-doping problem. This problem has been especially vexing for cases of especially high T_c in the absence of major formal doping. The ideas have led to the prediction of T_c increases by rational fractions. They have been subsequently experimentally realized. Given the success of these rules we search here for regularities concerning the placement of O^- in the structure either within a site or between sites. Basic considerations allow one also to draw inferences concerning the pair creation and its ordering within the CuO_2 plane (denoted Plane or P).

Within these concepts it is now possible to approach both the development of new materials and of questions concerning basic mechanisms in an uprecedented way on a rational chemical level. The encompassing perspective of these new concepts should also reflect themselves in the more complex physics of oxide superconductors. One aim of this study is to begin establishing this connection.

Development of the Anionic Model

A major breakthrough of the anionic model came with the prediction and subsequent experimental realization (1) of dramatic variability in the self doping of isostoichiometric $YBa_2Cu_3O_{6.5}$. A strong cell volume expanded form ($V+$) could be stabilized through a combination of special preparative techniques. This orthorhombic material, designated O3 for the uniform three-fold O coordination of Cu(1), corresponds to a high temperature modification. O3 can undergo rapid transition (4) to the conventional alternate chain (O42) modification and is usually not observed at room temperature. However, when it is stabilized, it undergoes V expansion (due to self doping) and exhibits about twice the T_c (extrapolated) of the conventional alternate chain modification (O42). It was explained based on self doping to $Cu(1)3^+$ and distribution of the holes to the total O lattice. This self doping occurs in order to ameliorate the developing stacking mismatch on cooling. In this particular case, self doping establishes stoichiometric holes of $h = 1$,

0022-4596/01 $35.00

corresponding to a doubling compared to the conventional O42 of h and T_c.

More generally, the proportionality of h and T_c was found to hold universally (2) in cuprate superconductors when calibrated to the total O content (y) according to $T_c = T_c^* r$ (radical formula) with $T_c^* = 666$ K and $h/y = r$ for some range of doping (see further below). In the definition of subperoxides O_q^{1-2q} with $q = y/h$ (e.g., $q = 7$ for $YBa_2Cu_3O_7$, as $h = 1$) one observes a trend to integer q and a T_c level scheme (e.g., T_c plateaus and maxima). This illuminates, for the first time, the "musical" or "quantized" nature of the T_c regularities.

Increases of T_c and h in response to changing lattice pressure have been generally invoked to explain the behavior of self-doped systems such as complex cuprates (e.g., based on Bi). Accordingly, they show a greater variability of T_c (e.g., maxima depending on preparation) compared with the well-developed "line T_c" of the ordered simple cuprates. Lattice pressure tailoring therefore holds a special promise for further increasing T_c.

General Aims and Aspects of Anionic Charge Order

The above indicates a new perspective for the theory of oxide superconductors as they quantitatively reflect properties expected for superconducting anionic charge order of O^- (SACO) (1–5). This pertains to the universal observation of their scaling of T_c with O^- radicals. The presence of O^- charge ordering also manifests itself in structural trends such as axial ratios. Aspects of these remarkable phenomenological rules indicate that T_c reflects quantitatively the p electron radical density on O in the usually assumed Cu($x^2 - y^2$)-O p hybridization, although Cu influences the fixing of the number of radicals. These ideas will be further extended to other anionic systems. It will be outlined that superconductivity is generally connected with the large, overlapping anionic sublattice in compound classes such as nitrides, carbides, or sulfides.

Generally, trends to subperoxide "quantization" O_q^{1-2q} are characteristic for the properties expected for one structure (charge order) within another (crystal). They reflect themselves in trends to specific T_c limits and levels (e.g., plateaus) in overoxidation or self doping within certain selection rules characteristic of the crystal structure. Also, O^- placement on selected crystallographic sites manifests itself directly in relation to structural detail and T_c. These experimental rules are in line with the ubiquitous observations of O^- in superconductors (6) and indications of O^-O^{2-} charge orders by diffraction experiments (7). The late realization of the full operation of these phenomenological rules had to do with the failure to discern between overoxidation and massive self doping. A direct consequence of the phenomenological rules is an understanding of the creation and annihilation of O^- through lattice pressure related factors. In fact, the focus of the chemical model on O^- creation as a slab mismatch remedy moves crystal chemistry to center stage in the understanding of the origins of the effects and utilization for materials development. This will be further elaborated.

However, the complex nature of Cu–O interaction and self doping can camouflage what is essential for superconductivity and what is not. For this reason, self doping in complex cuprates (based on M = Bi, Hg, Tl) is here excluded although it can be similarly dealt with. However, a comparison is drawn with related cases such as doped fullerenes (e.g., Rb_3C_{60}) (8). Common features with cuprates are a lattice of antibonding radicals. In this comparison, the presence of Cu and its adduct state properties are apparently not central to superconductivity. One aspect of this work will be to elaborate on the essential features leading to superconductivity and to search for common mechanistic elements and T_c energy scales. Several related anionic metallics such as Li_xHfN Cl (9) also are of interest as they offer instructive variations of the common theme. Again, there exist planar, infinitely extended, and contacting N^{3-} and Cl^- anions presumably with holes through self doping. In this sense, they are similar to the cuprates. However, due to their interdependent slabs they are not ideally suited for the purpose of elucidating the simplest common denominators. For a better understanding of the electronic nature of oxide superconductors, a brief introduction to essential features shall be given.

Details of Phenomenology

In the subperoxide model, the basic superconducting phenomenology can unfold in one of several modes (Table 1). One is overoxidation with a cationic–anionic equilibrium Ox

$$Cu_k^{2k+1}O^{2-} \rightleftharpoons Cu^{2+}O_q^{1-2q}.$$

Here, k and q are charge repeat wavelengths (e.g., $q = 7$ for $YBa_2Cu_3^{2+}O_7^{13-}$). An empirical relationship shows $T_c q = T_c^*$ that is, a universal constant. This indicates that equilibrium Ox is shifted somewhat to the right in the

TABLE 1
Compilation of Equilibria Creating and Destroying Subperoxides O_q^{1-2q} through Lattice-Pressure-Related Phenomena

Type	Equilibrium[a]	Representative example
Ox	$Cu_k^{2k+1}O^{2-} \rightleftharpoons Cu^{2+}O_q^{1-2q}$	$V-$, $YBa_2Cu_3O_7^{13-}$
Red	$Cu^{2+}O^{2-} \rightleftharpoons Cu_k^{2k-1}O_q^{1-2q}$	$V+$, $YBa_2Cu_3O_{6.5}$
Col	$O_q^{1-2q} \rightleftharpoons {}^cO^-$	C^-, e.g., $YBa_2Cu_3O_{6.7}$

[a] k and q are charge order repeat parameters and ${}^cO^-$ denotes occupation of O^- on c axis or apical site.

superconducting state. In addition, oxidation formally corresponding to $Cu^{2.5+}$ on the Plane ($k = 2$ or $h = \frac{1}{2}$ per Cu) appears to correspond to an energetic optimum which is not easily surpassed. It appears to be dictated by commensurability arguments and may limit T_c. O_q^{1-2q} are referred to as subperoxides with O_2^{3-} as the generating principle.

Beside the case of simple overoxidation, there exists massive self doping both in simple and complex cuprates. In this second mode, O^- is produced according to Red

$$Cu^{2+}O^{2-} \rightleftharpoons Cu_k^{2k-1}O_q^{1-2q}$$

through V expanding metal reduction. This equilibrium can also be seen as shifted to the right with trends to q or k "quantizations." This behavior can come into play as a result of thermal compression–tension on structural slabs developing on cooling (e.g., stratified tension doping within the five discernible states of $YBa_2Cu_3O_{6.5}$) (2, 3). It can also originate as a resonance with existing Ox (e.g., to double the holes or change q from 16 to 8 in $Bi_2Sr_2CaCu_2O_{8.25}$). The extent of the shift to the right in equilibria Ox and Red define the nature of an adduct state in which the Cu electronic system is drawn to O^- but not further oxidized. This shift can correspond to subperoxidic electronic liquefaction.

Antagonists to SACO are states in which different electronic properties arise through selective placement of h on crystallographic sites other than the planes. Examples are strong c axis decrease and T_c collapse (Col), which is here correlated with increased O^- placement on the spacer layer (BaO_2 related) rather than on the important CuO_2 plane.

A variety of diffraction experiments (see (10, 11)) indicate mobile charge ordering in superconductivity. Usually this reflects the lattice displacement by the charge modulation without special reference to the particular charges in question. Some techniques [7] however, appear now to pinpoint the charge carriers on the O. This is in line with the universal spectroscopic observation of O^- while Cu^{3+} is never observed. General thermodynamics is also in line with expectations (12) for the location of the O^{2-}–$|O^-$ couple and experimental observations such as O_2 evolution in H_2O on dissolving superconductors in dilute acid (13). This distinguishes cuprates from analog nickelates that are known to form stationary cationic charge orders, do not decompose H_2O, and have more stable Ni^{3+} thermodynamics (12). When pinned at certain commensurabilities (e.g., $\frac{1}{8}$ abnormality), stationary charge ordering can produce a striped nature of charge inhomogeneities (14). It is sometimes assumed (15) that these stripes are also characteristic for the superconductor although no consensus exists for a mechanism of pair propagation. Stripes are a natural consequence in the subperoxide model where subperoxidic charge channels $Cu_2^{2+}O_2^{3-}$ are embedded in a $Cu^{2+}O^{2-}$ matrix (3, 4).

From inelastic neutron scattering experiments (10) one finds a remarkably simple relation between T_c and the splitting of an incommensurate peak, or its half width d, with $kT_c = hu^*d$, where k, h, and u^* are Boltzmann and Planck constants and u^* is the velocity, respectively. This relates momentum to energy scales with u^* about a factor of 100 lower than u, the Fermi velocity. It was argued that the proportionality of T_c with d at slow u^* implies very slow moving, large-charged objects rather than electrons. It will be argued that those correspond generally to aspects of charge ordering of antibonding subperoxidic radicals.

Electronically, cuprate superconductors, above T_c, show abnormal linear resistivity–temperature behavior [16] for a metal, hinting at an unusual nature of their metallicity. For underdoped cuprates, a change in slope above a temperature T_p is observed in properties such as resistivity, specific heat, or magnetic susceptibility (17). This is usually referred to as the pseudo gap. Many properties characteristic of superconductivity come into existence already below T_p. This gap will be interpreted as O_4^{6-} pairing within a subperoxide stripe formation without full correlation among the stripes. Such correlation only happens below T_c.

Important electronic aspects of cuprate superconductors include the onset of Fermi surface related features (18) only along the plane diagonal on initial doping. On further doping, a full, somewhat distorted Fermi surface develops. On passing below T_c, the axial part dissolves but a diagonal part survives. This indicates that superconductivity is not propagating diagonally. Such behavior is in line with d wave property. However, recent studies indicate that stripe formation and superconductivity can be mainly one dimensional along an axis (19). A successful understanding of superconductivity must account for all these seminal findings. It will be shown that such an attempt on the subperoxide model leads to a unique and comprehensive new understanding of superconductivity. This understanding can be derived in part from basic materials principles.

RESULTS

In the following, selected aspects such as $T_c - r$ scaling, selfdoping, pair formation, and charge ordering will be worked out in the anionic model. Cuprates and related anionic superconductors will be compared. A picture will be developed for the temperature dependence of anionic charge ordering based on available experimental evidence. These features will allow a more comprehensive discussion for common elements in anionic superconductors.

Empirical T_c Relationship with Radial Concentration

A brief compilation of experimental data for simple overoxidized cuprates and related materials is given in Table 2. Selected examples are also presented in Fig. 1 (complex self doped cuprates based on Hg, Bi, Tl are omitted). T_c scales universally with radical densities per total O.

TABLE 2
Examples of T_c Catastrophes (Col) due to Preferential $^cO^-$ Site (Apical) Occupation and c Axis Contraction

Material	Diagnosis
C-, $YBa_2Cu_3O_{y,6.7}$	$c/3 \sim a = b$, no T_c, unbalanced oxide
$PrBa_2Cu_3O_7$	low c/p, correlates with absence of T_c
$LaCuO_3$	no T_c, low c/p
$(LaSr)_2CuO_4$	c axis slope changes after optimal doping
$Bi_2Sr_2Ca_2Cu_2O_8$	T_c and c axis reduction on overoxidation
$YSr_2Cu_3O_7$	Low T_c correlates with low c

There are no obvious exceptions within the constraints of the model (e.g., presence of Planes and absence of Col effects). The list given is representative for all relevant high T_c cuprate families, although special provisions must be made for self-doped complex materials with M = Bi, Tl, Hg. They pertain to self doping to limits of formal $Cu^{2.5+}$ on the Plane. It is assumed that a relationship of this type also

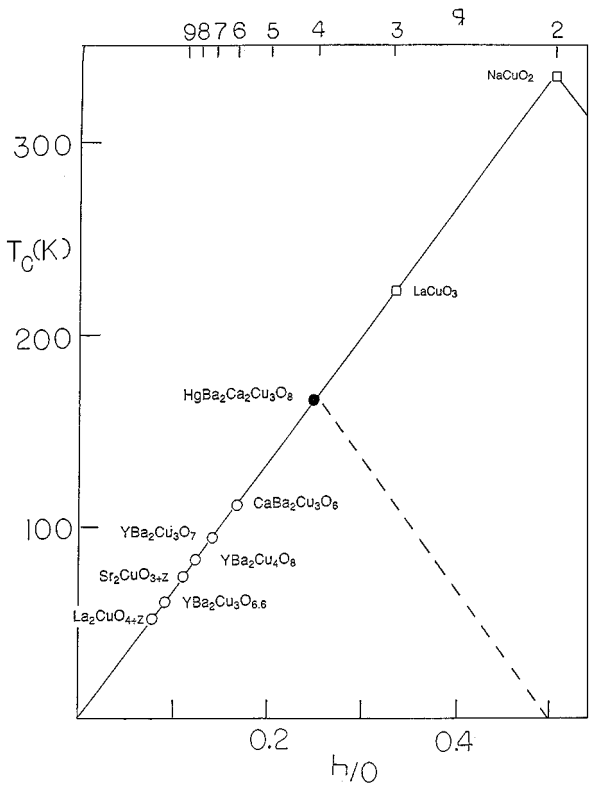

FIG. 1. Calculated T_c according to $T_c = T_c^* h/O$ with $T_c^* = 666$ K. Open circles correspond to selected simple overoxidized cuprate. Complex self-doped cuprates are omitted with the exception of $HgBa_2Cu_3O_8$ under pressure (bold). Experimental values for relevant, well-developed simple oxides fall within symbol size (e.g., other families with $q = 8$ such as $Pb_2Sr_2CaCu_3O_y$ with $y = 8$ also have calculated $T_c = 83$ K). There appear to be no exceptions. Squares are for fictitious superconducting materials and radical density decreases again for $h/O > 0.5$. T_c may universally decrease after reaching $k = 2$ on P (dashed).

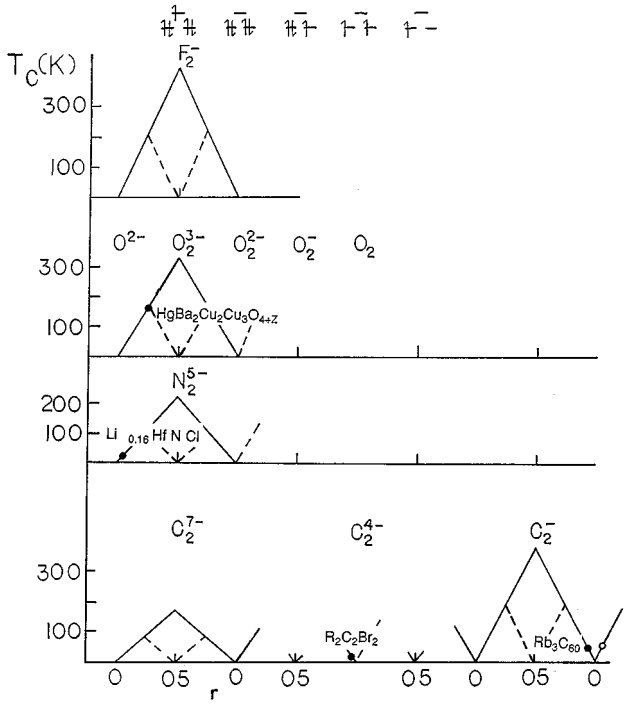

FIG. 2. Calculated T_c according to $T_c = T_c^* r$ and $T_c^* = 544$ en^2 for selected anions with increasing oxidation. The electronic states for relevant species are given on top. Accordingly, radical concentration is an oscillating function of oxidation and so is the theoretical T_c. Effective en increases for higher oxidation, indicating yet higher T_c for hypothetical O_2^- compared to O_2^{3-} type superconductors. This point explains that for Rb_3C_{60}, T_c^* appears similar to subperoxides although C has lower en. O is so far unusual in supplying especially high r. No superconducting halogen peranions are yet known. The T_c shown for the oxides corresponds to $HgBa_2Ca_2Cu_3O_{8+\delta}$ with pressure.

holds for related compounds such as Rb_3C_{60}. For $Li_{0.16}HfNCl$, the formal doping is well described ($h = 0.16$), but intriguingly, T_c (25 K) is twice the one of the similarly doped $Li_{0.16}Zr$ NCl, suggesting complex self-doping resonances.

General T_c Relationships

For understanding magnitude of T_c^*, we take the subperoxide bond energy as a relevant energy scale. We relate this to the electronegativity (en) according to $T_c^* = \text{en}^2$ constant. Calibrating to O with $T_c^*(O) = 666$ K, one calculates as an example $T_c^*(F) = 870$ K (Fig. 2). en is taken to correspond to the filled octet state while higher effective en values are assumed for lower electronic filling. For Rb_3C_{60}, q is 20 and $T_c^*(C)$ can be calculated near 700 K indicating that its effective en for C^{1-} is comparable to O^{2-}. Similar arguments pertain to related anionic superconductors (e.g., nitrides, borides). One generally expects that the linear relationship according to $T_c = rT_c^*$ peaks at maximum radical concentration. This is obtained for an oxidation state of

TABLE 3
Examples of T_c-q Families and Related Cases of Anionic Superconductivity

Material	h	q	T_c(K)	T_c(obs)[a]
$CaBa_2Cu_3O_{6+y}$	1	6	111[a]	(110)
$YBa_2Cu_3O_7$	1	7	95[a]	(92)
$YBa_2Cu_4O_8$	1	8	83[a]	(81)
$Sr_2CuO_{3+z(z\sim 0.16)}$	0.33	9	74[a]	(72)
$YBa_2Cu_3O_{6.6}$	0.6	11	61[a]	(60)
$La_2CuO_{4+z(z\sim 0.16)}$	0.33	12	54[a]	(50)
Rb_3C_{60}	3	20	33[a]	(33)

Note. h values are determined from stoichiometry and $q = y/h$. Similar behavior is found for similar q or y families. Examples are similar T_c for $q = 8$ for $Pb_2Sr_2CaCu_3O_{8+z}$ or $Bi_2Sr_2CaCu_2O_{8+\delta}$.

[a]See Ref. (2).

$O^{1.5-}$ or O_2^{3-}. Toward the peroxide O_2^{2-}, r and T_c will decrease to zero as all electrons are paired (see schematic in Fig. 2). In this range, h/y do not represent r anymore and the latter is therefore the more general parameter. However, further oxidation reintroduces radicals (rising even to $r = 1$ for O_2) and a potential T_c rise. Since effective en are higher for these higher oxidation states, maximum expected T_c should also be higher (higher T_c^*). This is also schematically presented in Fig. 2. Experimental realization of such a situation in contiguous network solids would require stabilization through highly electronegative components.

T_c Collapse as an O^- Placement Problem

The reduction of T_c beyond a certain doping is usually referred to as overdoping and explained as due to band filling effects. In addition, the absence of T_c in selected doped materials with planes is often not easily explainable. Here we indicate that both cases can be explained as a result of deleterious placement of O^- e.g., on the apical sites (Col). This manifests itself in dramatic reduction of the axial ratios. As an example, for $YBa_2Cu_3O_y$-type compounds the ratio c/p, where $p = 3(a + b)/2$, tends toward unity in the C-phase $YBa_2Cu_3O_{6.7}$. This is connected with the absence of T_c. Other examples are collected in Table 3. This effect can also set in gradually, e.g., with $(LaSr)_2CuO_4$ at relatively low T_c and with $(LaBa)_2CuO_4$ at higher T_c. In fact, for La_2CuO_{4+z} experimental values near the maximum calculated T_c (53*K) can be reached. This indicates that Col is not primarily reflecting a uniform band structure property connected with overdoping. It rather represents a crystal chemical feature of preferential O^- placement dependent on lattice pressure (e.g., small Sr has the most deleterious effect on T_c). It generally occurs on doping beyond the condition with $k \leq 2$ such as near the "ideal" structure in $YBa_2Cu_3O_7$. This structural imbalance represents the most severe limitation to the achievement of high T_c. The crystal chemistry of this ubiquitous calamity is discussed elsewhere in more detail (2, 4).

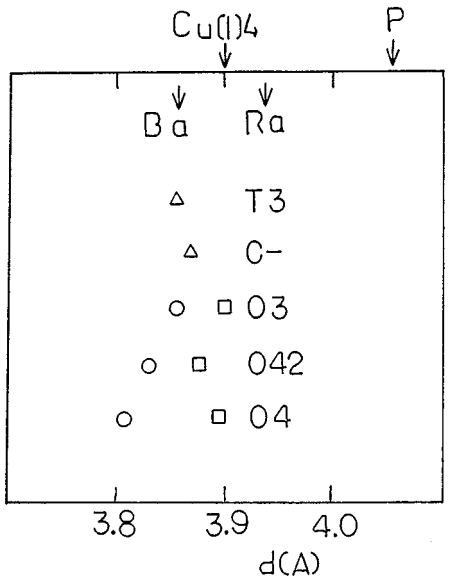

FIG. 3. Lattice matching in selected cuprates within a tolerance factor type picture. BaO and Cu(1)4 dimensions put P under compression leading to a tendency for subperoxidic electronic liquefaction. As shown in Fig. 4, the changing tolerance factor with temperature can lead to stratified self doping.

Tension Self Doping

We introduce now the basis for the self-doping model. Figure 3 shows the ideal BaO dimension ($d = 3.86$ Å) as measured along the CuO axis. The Cu (1)4 and P are also depicted. Accordingly, one notices that CuO bonds are generally under compression. They are therefore prone to subperoxidic electronic liquefaction which can shrink them. The experimental values depicted for selected cases generally reflect this contraction.

In the following we extend these ideas to the general behavior of stratified self-doping steps with temperature using the example of $YBa_2Cu_3O_{6.5}$. Conventional preparation establishes an orthorhombic with Cu coordination of 4 and 2 O, denoted O42. This results in cell volume contractions ($V-$). However, when materials in the transition region from tetragonal or orthorhombic are fast quenched, an O3 modification can be obtained (1). This can result in strong cell volume expansion phenomena ($V+$). The different doping types are presented in Fig. 4 in terms of different lattice pressure developing on cooling between the CuO_2 plane (Plane or P) and the charge balance (Balance or B, Cu (1) site) as outlined in more detail below. For $V-$ one obtains $h = 0.5$ in the conventional accounting. However, for $V+$ with $Cu(1)3^+$ one obtains $h = 1$ and doubled T_c (as observed on extrapolation of minutely Ni substituted

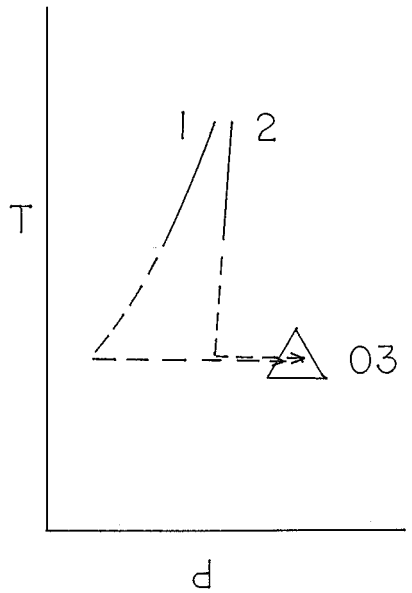

FIG. 4. Schematic of self doping as a result of different thermal expansion coefficients of two layers (1, 2). As their ideal lattice dimensions (d) diverge with lower temperature, internal electronic disproportionations can readjust slab fit. This can even employ V expansions (as shown). These tolerance-factor-type arguments hold the key to an understanding of self-doping stratifications and limits.

TABLE 4
Terms and Chemical Units in Subperoxide Charge Ordering

Term	Chemical units	Function or description
SACO	O_q^{1-2q}	Superconducting anionic charge order, q determines T_c
Adduct state	$Cu^{2+}O_2^{3-}$	Stabilizes holes without fully oxidizing Cu
Stripe	$Cu_2^{2+}O_2^{3-}$	Condenses holes in linear subperoxide wire
Ox	$Cu^{2+}O_q^{1-2q}$	Overoxidized equilibrium favoring $Cu^{2+}O_q^{1-2q}$
Red	$Cu_k^{2k-1}O_q^{1-2q}$	Reductive self doping
Col	$^cO^-$	T_c and c axis collapse due to selective placement of O^- on apical sites

materials). The strong basal plane expansions may argue for some V expanding Cu^+ on both Plane and Balance. At the same time, a smaller contribution of a V contraction type is assumed as due to "homogeneous" O^- formation. The latter is primarily responsible for the superconductivity. The phenomenology introduced above will now be used to construct an understanding on the chemical subperoxide model. It will involve plausible schemes for the changing charge order and transport as a function of temperature.

Pair Formation and Charge Ordering

In the following, we focus on the details of a most instructive case for the genesis of superconductivity, namely the conventional underdoped O42 material $YBa_2Cu_3O_{6.5}$ introduced above. A compilation of terms used is given in Table 4. This material obtains a stable tetragonal semiconductor T3, with only formal Cu^{2+}, upon synthesis in air. On relatively slow isostoichiometric cooling it transforms in a series of steps presumably first to a semiconducting O3 (see characteristic axial ratios) and then over some range of ladder compounds O342 to O42. The transformation to O42 occurs in a range around 400 K. It is seen as an adjustment of the Balance and the more space demanding P to the BaO layer. Subperoxide formation can shrink P and foster this adjustment. We assume initially disordered subperoxides O_2^{3-} for this state. Near $T_p = 200$ K the pseudogap opens. We take T_p to correspond to subperoxide pair formation in loose stripes of O_4^{6-} motifs. These pairs become fully correlated at $T_c \sim 50$ K. Figure 5 gives plausible renditions for correlated striped charge orders and pair formation below T_c. Figure 6 depicts the general electronic phase diagram of $YBa_2Cu_3O_y$.

In the following, arguments are presented for the choices in this rendition. We take strain energy and magnetic exchange to be responsible for the first organization of strings

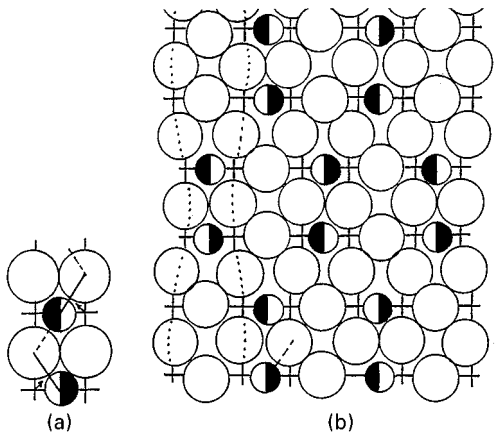

FIG. 5. (a) Schematic of possible subperoxidic pair formation on doping the CuO_2 planes. Crosses indicate Cu, large circles depict O, and shading indicates holes. Subperoxidic units O_2^{3-} are indicated. Pair formation is due to strain and bond polarization energies placing O^- pairs perpendicular to a CuO line, such that they can fit into the lattice. The assumed adduct state displacements of Cu (arrows) lead to two slightly different magnetic repeat distances as seen in diffraction. The assumed zig-zag charge propagation (pointed lines indicate new subperoxide) alternately expands and contracts the a and b axes and represents a pump mechanism for pair propagation. The actual charge order of subperoxide pairs will depend on details of lattice pressure. (b) Schematic of possible subperoxidic pair charge ordering with formation of charge channels. The alternate charge channel pattern as depicted corresponds to a universal oxidation limit ($k = 2$) that is not easily surpassed and may limit T_c. At lower doping, special stability of selected more dilute patterns (e.g., $k = 3$) can explain tendencies to T_c plateaus. Striping can be seen as a natural consequence of these trends.

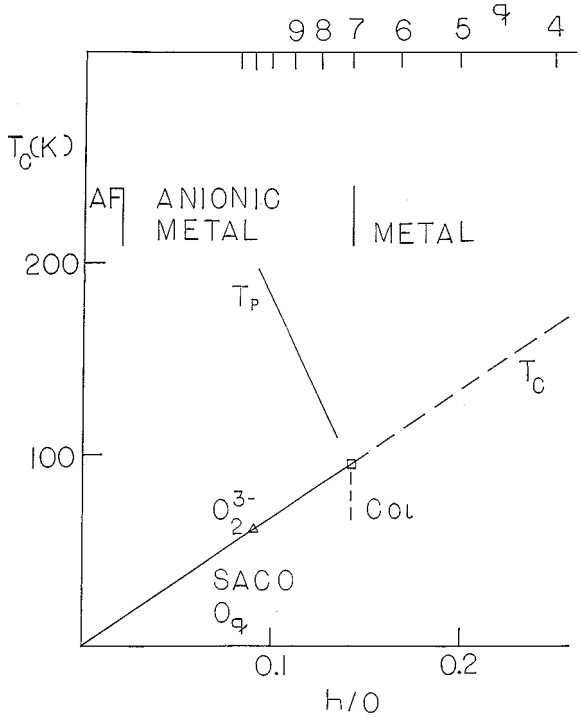

FIG. 6. Phase diagram for $YBa_2Cu_3O_y$ in the subperoxide interpretation, $y = 7$ corresponds to the square (T_c, 90 K plateau), $y = 6.6$ to the triangle (T_c, 60 K plateau). The superconducting paired charge order (SACO or O_q) breaks down above the universal linear $T_c(h/y)$ relationship into loose lines (subperoxidic stripes) of not fully correlated pairs (O_4^{6-}). Above T_p, O_2^{3-} subperoxide units become disordered. At still higher T, the materials can slowly transform to the thermodynamically stable forms (e.g., C^-). On overdoping, SACO breaks down in a T_c collapse (Col) where O^- placement becomes imbalanced and tends to apical site. A general distinction is made between the antiferromagnetic semiconductor (AF), the anionic metal, and the overdoped metal.

of O^- pairs. This stripe formation condenses the subperoxide pairs, such that they can fit into the crystal. This must happen along a line solely comprised of O^- pairs so that they can shrink while fitting into the lattice. If it were to involve Cu, a longer constricted segment could not be fit into the lattice. This is taken to be the reason for the occurrence of axial stripes in the cuprates as they are based on O^-. By comparison, diagonal stripes occur in the analog nickelates that are based on $Ni^{3+}Ni^{2+}$ charge order. O_4^{6-}-type clusters, moreover allow O spin pairing over intervening O. However, the attainment of full correlation is impeded by the large interstripe distance. Accordingly, $T_p > T_c$ in this hole concentration range. The full correlation below T_c utilizes bond polarization over all O. It is proportional to the radical density (see radical formalism). The striped nature appears to fade away for yet lower T (below T_c) and a more equidistant charge order of pairs appears to establish itself (the actual charge order will reflect details of lattice pressure). Such a charge order can also be assumed for the case of higher dopings which display no intervening stripe formation and have $T_c \sim T_p$ as in a BCS superconductor (the actual charge order may differ depending on lattice pressure). Patterns such as the one shown in Fig. 5 also produce two new magnetic $2a$ dimensions, in line with the presence of $2a \pm x$ spots in the diffraction pattern. The slow propagation of large charged objects (rather than electrons) suggests that aspects of the whole charge order are involved. The details of this propagation are also depicted in Fig. 5.

The basic assumptions are that pair formation takes place through strain energy and bond polarizations of an indirect exchange type (see short coherence length). In addition, local V expansion ($V+$) and contraction ($V-$) waves provide a push–pull mechanism for the propagation and coupling among pairs. The adduct state Cu direct the propagation into zig-zag channels and impart d-wave characteristics. This allows for spatial equilibration and adjustment that is taken as the main driving force for the electronic liquefaction.

DISCUSSION

The discovery that the experimentally observed O^- in superconductors manifest themselves in structural trends, and a universal T_c scaling with radicals per O (or the Cu | O ratio) supplies a crucial element in the debate about the origin of T_c. The principal involvement of O^-, in fact, is even seen (20) in the spectroscopy of compounds such as $NaCuO_2$ and is rooted in its thermodynamics. Thermodynamically selected elements such as Cu can have a stabilizing influence for subperoxide formation. We will now outline how the complex and often contradictory phenomenology can be brought under a common conceptual roof when based on O^-.

A wealth of experimental information can now support the notion that high T_c superconductivity is primarily connected with a charge order of self-bonding anionic radicals either in oxides or related high electronegativity materials. A linear T_c scaling with holes has been realized early on and it was found to have different slope for different families (Uemura plot (21)). However, this dependence has now been shown (2) to be of a universal character when represented on an O^- radical density (per total O). It pertains both to overoxidation and self doping. Also, limits and levels of T_c reflect characteristic trends, pointing to special charge order commensurability constraints. Experiments indicate that $h/n = \frac{1}{2}, \frac{1}{3}$, etc. are arrangements of special stability on the Planes (n corresponds to number of P). Indications for anion charge ordering have now also appeared independently in diffraction experiments (7). Also, the involvement of O^- provides a first quantitative answer to the self-doping question and an encompassing view in which formal n and p doping are both based on O^- holes (see the common feature of p holes in the Fermi surface). Furthermore, selective O^- placement explains aspects of overdoping as

a crystal chemical calamity. It is therefore not accepted as a universal band feature but can be counteracted by crystal chemical means. Also, the involvement of a new type of self-bonding anionic resonance hybrid appears plausible, which is based on CuO adduct state polarizations. Properties such as stripes are more naturally explained on O^-, avoiding space filling difficulties with Cu^{3+} in the geometry along an axis. Within these concepts it is now also possible to draw inferences concerning aspects of the actual charge ordering. Even the actual geometries, mechanisms, and energetics of pair propagation become tangible.

For the cuprates, the slow charge propagation implies large charge objects such as aspects of the charge order (e.g., correlated subperoxide pairs) rather than electrons. The sensitivity of T_c on all O indicates that all O participate in one or another way in charge propagation. This appears to involve polarization of the total O resonance hybrid. This is seen as a shift of p electron density from all O toward the subperoxide bond. The dependence of T_c on the massive number of all stoichiometric holes also suggests that aspects of the whole electron paired charge order move in a correlated way. Accordingly, strong correlation effects within the O bond system are at the heart of a detailed energetic understanding. A system of resonating antibonding radical bonds appears indicated, and polarization effects within the total bond system will have to be worked out. It is satisfying to see that it is possible to construct schemes based on the anionic model which appear to be generally in line with the complex evidence to date.

A similar situation can be assumed for other electronegative elements. Accordingly, peranion formation of antibonding radicals and a scaling of T_c with their density (and predilection for certain q) are universally expected. For the fullerenes it is likely that considerably higher T_c could be obtained if one could force higher doping levels. In fact, $q = 20$ for Rb_3C_{60} is still disadvantageously large by comparison with the cuprates. In the case of the fullerenes, orbital overlap can be assumed for both n- and p-type doping. Both supply local $V+$ effects through bond weakening. In this exceptional case, cationic charge orders should also lead to superconductivity. In geometries where cationic charge order cannot overlap, the chance for superconductivity should be diminished.

Antibonding radicals can also be assumed for T_c in $Li_{0.16}HfNCl$ through internal disproportionation to N_q^{-3q+1} and reduced positive charge on Hf. In fact, a self-doping resonance can be assumed, in analogy with compounds such as $Bi_2Sr_2CaCu_2O_{8.25}$ as it has twice the T_c of the analog $Li_{0.16}ZrNCl$. Elsewhere, we point out (5) that anionic superconductors (e.g., carbides, nitrides, sulfides ($PbMo_6S_8$), or hydrides (Th_4H_{15}, PdH)) display radial ratios of anion to cation uniformly near 2. This represents a condition for hard sphere contact between the anions and therefore for anionic metallicity and superconductivity. Slab or bond mismatch stress generates peranion principles (e.g., O_2^{3-}, N_2^{5-}). Their kinetic distribution restores the integrity of the structure.

However, the remarkable T_c of the fullerenes appear not to depend on interacting layers or magnetic exchange. The most basic common denominator for superconductivity accordingly is the presence of radicals that appear to be in the state of a traveling charge order. The electron correlation energetics are therefore directly related to energies stabilizing the charge order and basically represent a crystal chemical bonding question. In the following, this will be discussed in more detail.

There appear to exist characteristic differences between the traveling anionic charge order of cuprate superconductivity and the cationic charge orders of, say, the doped nickelates. Charge mobility is severely limited for the stable $Ni^{3+}Ni^{2+}$ arrangement due to the lack of contact of the small Ni ions and the difficulty to propagate over the Ni–O bonds. These materials therefore do not become matallic at comparable doping levels to the cuprates. However, for cuprates, O^- is observed while Cu^{3+} is not, and the direct contact of O in diagonals suggests a path for metallicity. Accordingly, a Fermi surface-like feature establishes itself indeed first along the diagonal on initial doping. The relevant charge carriers can be assumed to correspond to disordered subperoxidic diagonal trains.

At increasing doping levels a slightly distorted, full Fermi-surface-like feature develops. Below T_p indications are for axial charge propagation. This is related to the formation of O_2^{3-} subperoxidic pair. They extend along stripes based on CuO adduct states. The origin of this first charge ordering below T_p apparently has to do with a formal local phase separation between the subperoxide and the $Cu^{2+}O^{2-}$ insulator. This appears to reflect the stress between plane and spacer layers. It will also reflect the short range order in the magnetic background. T_p scales negatively with h, which dilutes the magnetic interaction and is therefore irrelevant to T_c. In this picture, superconductivity makes use of stripes only as a template and does not use them altogether at high doping.

The first organization of the subperoxidic charge trains below T_p reminds one of aspects of superconductivity. It has, however, not yet correlated the CuO_2^{3-} motion. This correlation appears below T_c that scales positively with h. It is considered to reflect local strain and O polarization energies. In this way, a classical material or chemical-type picture emerges for superconductivity. It represents the natural progression in the correlation of stress mediating mobile radical bonds. The relevant short range interactions (low coherence length) make use of strain and bond energies which are powerful enough to explain the theoretical limit of $T_c = 333$ K or 167 K for the subperoxides.

Pair propagation was considered early on, albeit along O diagonals (22). It was not based on the linear h/y-T_c

scaling or the involvement of a charge order coupled through resonance hybrids on O as proposed here. Energetic questions of pairs on Cu, moving perpendicular to assumed Cu charge stripes, have also been worked out (15).

Elsewhere (4, 12), we discuss in more detail that shifts favoring the subperoxidic state in the adduct equilibrium correspond by and large to metastable situations. They indicate escape routes from thermodynamically frozen situations ameliorating the developing thermal stress on cooling. Accordingly, one understands that the anionic metallicity drives the stress mismatch in the form of incipient phase separation through the crystal. Given a favorable structure but marginal metal thermodynamics for subperoxide adduct states (e.g., Ni based), one can expect that strong lattice pressure may in principle also induce a wider range of materials to become black superconductors. Resistivity anomalies (23) for thermally stressed $(La_{2-x}Sr_x)_2NiO_4$ may be an example. These ideas can generally lead to a variety of predictions (4) concerning T_c increases. Any strong internal slab mismatchings such as achievable through quenching, in artificially layered films, or through mechanical deformation (e.g., bending) are promising with respect to an increase in structure ameliorating self doping. A variety of reports of high T_c anomalies may be due to effects such as surface tension and as such important for further materials development.

The newly worked out concepts can provide some remarkable new perspectives for the solid state. They include a fuller realization for the existence of a new class of materials, namely, the anionic metals, characteristic for the electronegative corner of the periodic table. These black metals with their uniform radial ratios, ensuring anion overlap, are dramatically different from their cationic counterpart. A most general principle of structural adaptation is identified for metallic solids. This pertains to stratified overoxidation or self doping and concomitant electronic liquefaction to ameliorate the internal stresses. This electronic liquefaction presents an alternate route to structural stabilization to the well-known class of infinitely adaptable structures (see e.g., (24)). Its realization promises the beginning of crystal chemistry of peranion formation.

CONCLUSION

The involvement of O^- and its anionic charge ordering can provide a comprehensive and self-consistent new perspective for a quantitative understanding of oxide superconductivity. It is seen in a variety of distinctive aspects such as:

The universal scaling of T_c with O^- radical density;
The self doping of $V+$ analogs under basal plane expansion which cannot be explained by conventional Cu^{3+} doping;
The ubiquitous connection of the placement of O^- on apical sites with the collapse of T_c (Col).

The benefits of this new perspective include:

An understanding of pair formation and propagation on crystal chemical grounds;
The promise of a crystal chemistry of O^- creation based on lattice pressure;
Predictive capabilities and a unified model for superconductivity.

These discoveries present an unprecedented promise for the development of leading edge materials and an understanding of basic mechanisms. They severely restrict the number of factors responsible for superconductivity to self bonding related concepts and add an affirmative note to the cumulative indications that charge-order-related features, albeit subperoxidic ones, have to do with superconductivity. A comparison with related anionic metallics is indicated. A common feature between cuprates and related materials is the presence of radical bonds that are prone to travel. Their coupling through strain energy or bond polarization related parameters lead to electron correlations needed to explain the slow propagation of an anionic charge order of subperoxidic pairs. The so far underestimated anion dictates a major part of the phenomenology and the deeper meaning of this has yet to be explored.

REFERENCES

1. D. Ko and H. Oesterreicher, *Physica C* **277,** 95 (1997).
2. H. Oesterreicher, *J. Alloys Comp.* **299,** 264 (2000).
3. H. Oesterreicher, Proceedings, MOS Stockholm 1999, *J. Low Temp. Phys.* **117,** 993 (1999).
4. H. Oesterreicher and J. O'Brien, *J. Alloys Comp.* **306,** 96 (2000).
5. H. Oesterreicher, unpublished manuscript.
6. B. Raveau, "Crystal Chemistry of High T_c Superconducting Oxides," Springer-Verlag, Berlin/New York (1991).
7. Y. Petrov and T. Egami, *Phys. Rev. B* **58,** 9485 (1998).
8. S. H. Irons *et al.*, *Phys. Rev. B* **52,** 15517 (1995).
9. S. Yamanaka, K. Hotehama, and H. Kawaji, *Nature* **392,** 582 (1998).
10. A. V. Balatsky and Z. X. Shen, *Science* **284,** 1137 (1999).
11. B. O. Wells *et al.*, *Science* **277,** 1067 (1997).
12. H. Oesterreicher, *J. Alloys Comp.* **267,** 66 (1998).
13. H. Oesterreicher and D. Ko, *J. Alloys Comp.* **269,** 246 (1998).
14. J. M. Tranquada *et al.*, *Superconductors* **9,** 397 (1996).
15. V. J. Emery and S. A. Kivelson, *J. Low Temp. Phys.* **117,** 189 (1999).
16. B. Batlogg, *Physics Today* **44** (1991).
17. H. A. Mook *et al.*, *Nature* **395,** 580 (1998).
18. P. Coleman, *Nature* **392,** 134 (1998).
19. H. A. Mook, P. Dai, F. Dogan, and R. D. Hunt, *Nature* **404,** 729 (2000).
20. T. Mizokawa, A. Fujimori, H. Namatame, K. Akeyama, and N. Kosugi, *Phys. Rev.* **49,** 7193 (1994).
21. Y. J. Uemura, *Phys. Rev. Lett.* **62,** 2317 (1989).
22. J. Hirsch, *Physica C* **158,** 326 (1989).
23. K. S. Nanjundaswamy *et al.*, *Physica C* **166,** 361 (1990).
24. P. Rabus, A. Meerschaut, J. Rouxel, and A. G. Wiegers, *J. Solid State Chem.* **88,** 451 (1990).